

A Systematic Geophysical Approach for Site Response of the Dinar Region, Southwestern Turkey

ALI ISMET KANLI¹, TAE-SEOB KANG², ALI PİNAR¹,
PÉTER TILDY³, and ZSOLT PRÓNAY³

¹Department of Geophysical Engineering, Istanbul University, Istanbul, Turkey

²Earthquake Research Center, Korea Institute of Geoscience and Mineral Resources, Daejeon, Korea

³Department of Engineering Geophysics, Eötvös Loránd Geophysical Institute, Budapest, Hungary

On 1 October 1995, the Dinar earthquake (M_w 6.1) devastated the city of Dinar in southwestern Turkey. We investigated the effects of geological conditions on the localized damage patterns using microtremor survey and multichannel analysis of surface waves. The microtremor survey was carried out in and around the Dinar basin to determine the resonance frequencies and depths of the sedimentary layer at 38 different locations using a broadband seismometer. The shear-wave velocity profile of the basin sediments was estimated from the inversion of the microtremor horizontal-to-vertical spectrum based on surface waves from seismic noise at each site using a genetic algorithm. The average shear-wave velocities estimated from the multichannel analysis of surface waves experiments were given as constraints in the inversion. A new relationship between the thickness of basin sediment and the main peak frequency in the horizontal-to-vertical spectral ratios was derived. This relationship allows a zonation of the Dinar region, which is consistent with previous studies and can be importantly used for the seismic hazard evaluation of the region.

Keywords Site Response; Dinar City; Microtremor Survey; Multichannel Analysis of Surface Waves; Horizontal-to-Vertical Ratio Inversion; Genetic Algorithm

1. Introduction

The town of Dinar, which is built on a soft alluvium basin, was hit by a moderate earthquake (M_w 6.1) on October 1, 1995; the hypocenter of the event was located just beneath the town (Fig. 1). Despite its moderate size, the impact of the earthquake was large and about 20% of the buildings collapsed or were damaged beyond repair [Durukal *et al.* 1998; Ansal *et al.*, 2001].

The spectral content of accelerograms recorded by instruments deployed on sites with different geologic features identified a very distinct relationship between the damage distribution and the near surface geology. In terms of this relationship, the city could be divided into three different zones (Fig. 1): a hillside region underlain by firm rocks where no or light damage occurred (zone I), a transition zone covered by a few meters to a few tens of meters of unconsolidated material where the damage was moderate (zone II), and the region of heavy damage located on the Dinar basin where the sediment thickness

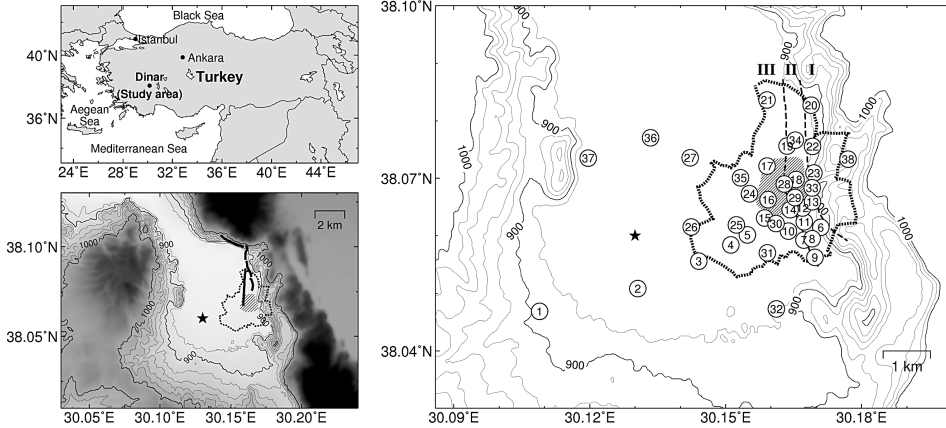


FIGURE 1 Regional map showing the study area and topographic map of the Dinar region with contours in meters (left). The locations where microtremor measurements were made are shown with numbered circles (right). Dashed lines represent the boundaries between the zones indicated by roman numbers: the (I) hillside, (II) transition, and (III) basin zones. The star indicates the epicenter of the October 1, 1995 earthquake from Wright *et al.* [1999], and the thick solid lines denote the traces of surface rupture. The boundaries of Dinar are indicated by the dotted line and the area of heavy damage is shaded.

reaches up to 250 m (zone III) [Özpinar, 1978; Kayabali, 1997; Durukal *et al.*, 1998; Ansal *et al.*, 2001].

A tremendous amount of geotechnical data has been collected in Dinar, including drilling, conic penetration, seismic refraction, geoelectrical, and microtremor measurements. These demonstrated that the main factors controlling the damage distribution were the local site conditions and soil amplification, due to the geological and geotechnical features [Turker *et al.*, 1996; Ansal *et al.*, 2001]. Kayabali [1997] computed the predominant periods of the sediment columns at different sites and concluded that the near-surface geological conditions did not have a great effect on the observed damage distribution, while poor designs and inadequate building materials played a key role, together with the long duration of the earthquake.

The starting points and objectives of our microtremor study carried out in Dinar and its surroundings can be briefly outlined as follows. First, as in most microtremor studies, Ansal *et al.* [2001] carried out a study using short period seismometers whose natural periods are about 1 Hz, a frequency range that is wide enough for most engineering purposes. However, the spectral content of the seismograms acquired with short-period instruments usually lacks the lower frequencies that include the predominant periods of thicker sediments. Therefore, to avoid this problem, we used a broadband seismometer. Second, the shear-wave velocity profile of the basin sediments was estimated by inverting the microtremor horizontal-to-vertical (H/V) spectrum based on surface waves from seismic noise at each site using a genetic algorithm. The average shear-wave velocities estimated from the multichannel analysis of surface waves (MASW) experiments are given as constraints in the inversion. Finally, in an attempt to unravel the cause of the devastation in Dinar, we compared both the lateral variation of the resonance frequencies and the results from the ground motion synthetics with the damage distribution associated with the 1995 Dinar earthquake.

2. Site Description and Microtremor Measurements

The Dinar basin is an intermountain graben a few kilometers wide within an extensional regime in western Turkey (Fig. 1). The basin is filled with Pliocene-Quaternary unconsolidated sediments of pebbles, sand, silt, and clay, and the mountainous region consists of relatively old limestone, flysch, and conglomerate, which is considered bedrock. Numerous geophysical and geotechnical experiments have examined the properties of the subsurface soil in the basin [Özpinar, 1978; Turker *et al.*, 1996; Ansal *et al.*, 2001; Bakir *et al.*, 2002]. A resistivity survey by Özpinar [1978] showed that the basin depth exceeds 200 m. A seismic refraction survey provided shear-wave velocity profiles to a soil depth of 20 m in the Dinar basin [Turker *et al.*, 1996] and the results from the MASW study showed that the soil has relatively low shear-wave velocities between 150–240 m/s [Kanli *et al.*, 2004, 2006]. These features imply that a considerable impedance contrast exists at the sediment-bedrock interface. Bard and Chávez-García [1993] showed that both the deeper and shallow layers have a strong effect on the surface ground motions. Consequently, ground motions are significantly affected by the impedance contrast at the sediment-bedrock interface [Street *et al.*, 1997; Cardenas-Soto and Chávez-García, 2003]. However, the lack of velocity information for all the sediments down to bedrock in the Dinar region makes it difficult to assess the site responses and the damage distribution during the October 1, 1995 earthquake.

Microtremor data were collected from 38 sites located in Dinar and its vicinity (Fig. 1). The data were gathered using a Guralp CMG-40T three-component broadband seismometer that had a flat velocity response between 0.03 and 50 Hz. The sampling rate was 100 Hz. Most of our microtremor measurements were made in the parts of Dinar that were heavily damaged during the 1995 Dinar earthquake, in order to look for a relationship between the resonance frequencies and damage distribution. We also made measurements outside the city to investigate the lateral variation in the Dinar basin.

We investigated the frequency content of the seismograms as a function of time to determine how the instrument is affected by temperature changes, and found that the frequencies lower than 0.2 Hz are primarily influenced. Using a similar seismometer, Bodin *et al.* [2001] took measurements at the surface and compared them with ones recorded in holes about 50 cm deep and noticed that the noise at periods of over 5 s was lower.

In order to obtain the spectral H/V ratio for each noise recording, we selected 15 data windows with a duration of 81.92 s each, with no spikes. Any trends or DC offset were removed and 10% symmetric cosine tapering was applied. After the Fourier amplitude spectra of the vertical and horizontal components of the 15 data windows were calculated, the spectra were smoothed using a five-point Hanning window not affected by the location of the resonance frequency. The spectral ratio of the horizontal to vertical components for each window was computed and averaged over all 15 data windows. Nineteen of the 38 measurement sites were located in the basin region, 11 sites were located in the transition zone, and 8 sites were located in the hillside region (Fig. 1). Samples of typical spectral ratios obtained from these three regions are illustrated in Fig. 2.

3. Shear-Wave Velocity Profiles from Inversion of the Microtremor Data

The evaluation of site effects requires information on the velocity structures of the sedimentary layers overlying the bedrock. First, the MASW technique was used to determine the structure of the near-surface sediments at each microtremor site. This method involves measuring the surface wave dispersion curve along a seismic recording

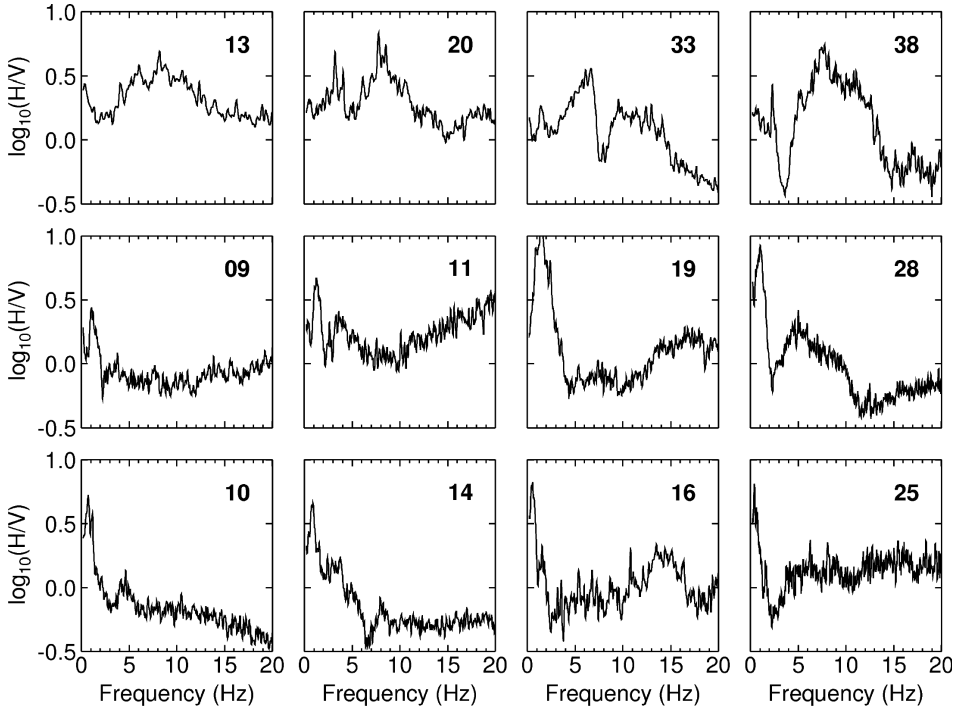


FIGURE 2 Examples of horizontal-to-vertical (H/V) spectral ratios obtained from the hillside (zone I, top row), transition (zone II, middle row), and basin (zone III, bottom row) zones. The numbers indicate the locations where microtremor measurements were made, as shown in Fig. 1.

profile and interpreting it to obtain the corresponding shear wave velocity. We used 24 2.5-Hz geophones spaced at equal 4-m intervals to record the surface waves. We used a seismic source capable of producing long wavelengths. In order to obtain the near-surface velocity profiles at each site, the dispersion curves of Rayleigh waves were inverted using a genetic algorithm. The resulting layer thickness and velocities were used to calculate the average shear-wave velocity at depths up to 30 m [Kanlı *et al.*, 2004, 2006; Fig. 3A]. Although it is a key study to calculate the average shear wave velocity of the upper 30 m (v_s^{30}) for the soil classification studies according to the Uniform Building Code (UBC) [Dobry *et al.*, 2000; Kanlı *et al.*, 2006] and Eurocode standards [Sabetta and Bommer, 2002; Sêco e Pinto, 2002; Kanlı *et al.*, 2006], the penetration depth is limited by the low energy of the loading source, which prevents an examination of the deeper sediments or bedrock. When the depth to the sediment-bedrock interface exceeds the penetration depth with the MASW technique, we must perform further work to estimate the average shear-wave velocity of the sedimentary layer.

The longer wavelength of microtremor energy allows the traveling waves to penetrate deeper. Recent studies have shown that the microtremor H/V spectrum can be modeled successfully using the theoretical H/V spectrum of surface waves depending on the shear-wave velocity profile down to the bedrock [Arai and Tokimatsu, 2004; Parolai *et al.*, 2005]. The theoretical formulas consider the effects of the changes in the fundamental and higher modes of both Rayleigh and Love waves with frequency. Then, we can estimate the shear-wave velocity structure by inverting the microtremor H/V

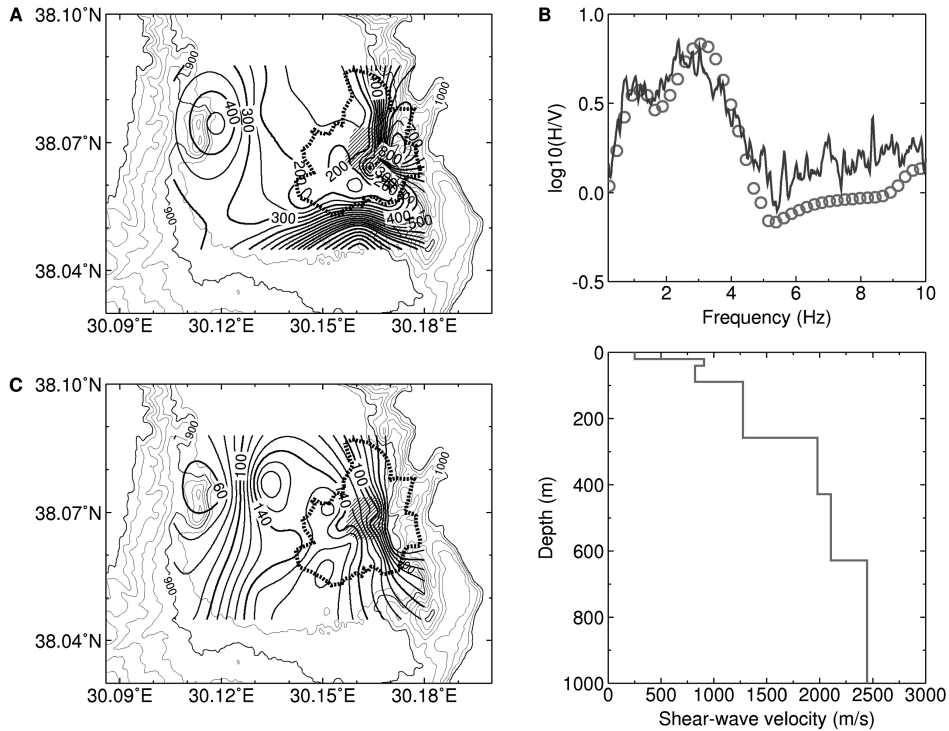


FIGURE 3 (A) v_s^{30} (m/s) distribution from MASW experiments. In each microtremor measurement site, the corresponding v_s^{30} value is used as initial constraints for the inversion of the microtremor H/V spectrum ratio. (B) Example of an inverted microtremor H/V spectrum for shear-wave velocity profiling. The top panel compares the H/V spectrum of a microtremor (solid line) with synthetic data (open circles) for the inverted shear-wave velocity profile at site 1 given in the bottom panel. (C) Lateral variation in the sediment thickness (m). The contours are given at an interval of 10 m. The other symbols are the same as in Fig. 1.

spectrum at a site. This is accomplished by minimizing the misfit between the measured and theoretical H/V spectrum for several stratified layers over half space. However, the resulting profile involves a trade-off between the layer thickness and average layer velocity occurring in the inversion process [Scherbaum *et al.*, 2003]. In this study, the average shear-wave velocity (v_s^{30}) estimated from the MASW experiments in Fig. 3A can be used as a constraint when inverting the microtremor H/V spectrum.

The propagator matrix method is used to formulate normal mode solutions for surface waves following Harkrider [1964]. Then, the theoretical H/V spectrum of surface waves is described as the ratio of the horizontal power spectra of the Rayleigh and Love waves to the vertical spectrum of the Rayleigh waves [Arai and Tokimatsu, 2004]. The ratio between the horizontal and vertical microtremor loading forces on the ground is fixed at unity following the test results of Parolai *et al.* [2005]. The forward calculation considers the higher modes and fundamental mode of the surface waves for the amplitude spectra representing the medium responses. In addition, the H/V ratios of Rayleigh waves on the free surface are calculated in the corresponding modes.

The inversion is carried out using a genetic algorithm that does not depend on the explicit initial model [Carroll, 1996]. For the inversion, we defined several elastic, homogeneous, and isotropic layers with half spaces that are characterized by their thickness (h), density (ρ), and compressional- and shear-wave velocities (v_P , v_S). Previous studies have shown that the thickness and shear-wave velocity at each layer are the predominant parameters governing the theoretical H/V spectrum (e.g., Satoh *et al.*, 2001; Arai and Tokimatsu, 2004). Therefore, we focused on both of them as model parameters to be estimated in the inversion process. The compressional-wave velocity of each layer is obtained from the shear-wave velocity using the empirical relations $v_P = 920.80 + 2.61 v_S$ for $v_S \leq 400$ m/s and $v_P = 1677.7 + 0.72 v_S$ for $v_S > 400$ m/s, and mass density $\rho = 1570.32 + 0.31 v_S$, where the units are SI units. The relationships are simply obtained from the linear regression of the results of the MASW experiments.

We estimated the shear-wave velocity and thickness of the horizontal layers composing the subsurface structure at 38 sites to match the theoretical microtremor H/V spectrum to the observed one. The model is divided into six layers and half space. The thickness of each layer is freely variable within the range of 0.1–300 m for the 3 top most layers and 0.1 – 1000 m for the other three layers during the inversion process using the genetic algorithm. The parameter space of the shear-wave velocity for each layer is within 2.0 km/s and the half space has the maximum velocity for the entire model. For the top layer, the results estimated from the MASW experiments (Fig. 3A) are used as initial constraints for the inversion. After the 50th iteration, the resulting parameters with the best fit for the calculated H/V spectrum to the observed one are selected as the optimal model. If the resulting parameters are on the bound of the parameter space where model parameters are allowed to vary, another 50 iterations are followed with modification of the parameter space.

Figure 3B shows some examples of the inversion. The calculated H/V spectra are in fairly good agreement with the observed spectra. In order to estimate the range of sediment overlying the bedrock, we examined the velocity contrasts between the layers from the velocity model showing the best fits. We selected the estimated thickness of the first layer or up to the second layer as the range of sediment overlying the bedrock while considering the large velocity contrast between sediment and bedrock. Since this is a rather subjective conjecture, we checked the validity of the estimated sediment depths by comparing them with the ones estimated from a resistivity experiment Özpınar [1978] conducted in the Dinar basin. Our estimates of the depth to bedrock were very close to the estimates from the resistivity experiment. Therefore, we determined the depth of the sedimentary layer beneath each observation site and constructed a map showing the lateral variation in the depths, as illustrated in Fig. 3C.

4. Relationship between Resonance Frequency and Sediment Thickness

The spectral H/V ratio of each measurement location enables an estimation of the resonance frequency at that site. We made a visual selection of the resonance frequency for each ratio. Figure. 4A shows a spatially interpolated map of resonance frequencies covering the entire study region. The resonance frequencies at the 38 sites where microtremor measurements were made ranged from 0.3–12.0 Hz and the estimated depths to the bedrock varied from 10–220 m. The average shear-wave velocity range was also quite wide and varied between 170 and 480 m/s. The main reason for such a wide range of results arises from the large differences in the near-surface geological conditions of the basin, transition, and hillside regions. Some investigators who have applied the microtremor method have claimed that this method is only valid for regions where a large

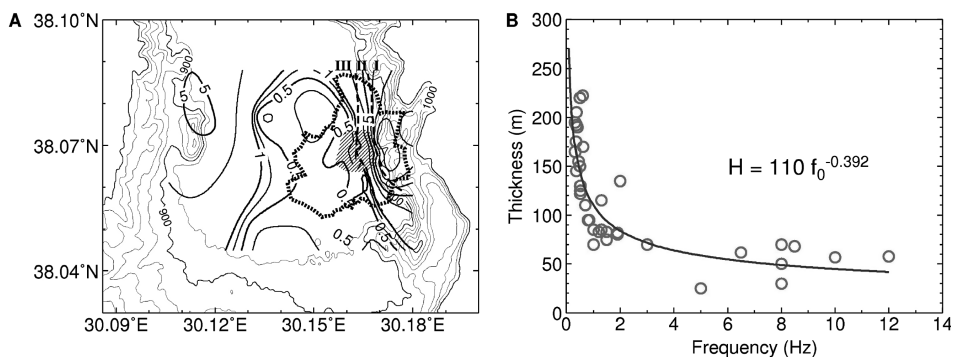


FIGURE 4 (A) Lateral variation in the resonance frequencies (Hz). The contour values higher than 1.0 Hz are given at an interval of 2.0 Hz, and the contour values smaller than 1.0 Hz are given at an interval of 0.25 Hz. Dashed lines represent the boundaries between the zones indicated by roman numbers, which are described in Fig. 1. (B) The relationship between the resonance frequency and sediment thickness in the Dinar region.

impedance contrast exists between the soil and underlying bedrock (e.g., Luzon *et al.*, 2001). However, we found that this method could be used successfully at sites not necessarily overlain by a soil layer. The necessary and sufficient condition is to have an impedance contrast between the upper and lower layers. For example, we had several measurement sites on the hillside of Dinar overlain by stiff material where the resonance frequencies were much higher than in the basin and transition regions. The plots of resonance frequency versus sediment thickness derived at the hill sites fit the estimates for the basin and transition zones reasonably well. This is illustrated in Fig. 4B, in which we derive a relationship between the resonance frequency (f_0) and thickness (H) of the overlying layer, which is given as $H = 110f_0^{0.392}$.

The f_0 - H relationship states that if we know the resonance frequency of a site, then the thickness of the overlying layer can be estimated. It remains to be determined whether this relationship can be used in other basins. Previous studies suggest that such a relationship is representative for basins of similar type or age. For example, Parolai *et al.* [2002] and Ibs-von Seht and Wohlenberg [1999] obtained relationships of $H = 108f_0^{1.551}$ and $H = 96f_0^{1.388}$, respectively, for different basins in Germany. The coefficients differ somewhat from those in our study. We postulate that the difference in the relationships derived for the Dinar and German basins results from the age or rate of tectonic activity forming the basins. In fact, we observed an interesting feature in our H and f_0 maps (Figs. 3C and 4A, respectively) that fuels our speculation. The north-south oriented surface ruptures that occurred in Dinar nearly parallel the north-south trending contours of both the resonance frequency and sediment thickness. We believe that this pattern is directly related to the presently active normal faults forming the Dinar basin. Therefore, we believe that the sediments accumulated in the Dinar basin are much younger than those of the German basins, resulting in the different $f_0 - H$ relationships.

5. Discussion and Conclusions

In terms of the distribution of damage associated with the 1995 Dinar earthquake, Dinar can be divided into three regions: the hillside, transition, and basin regions (Fig. 1) [Durukal *et al.*, 1998; Ansal *et al.*, 2001; Bakir *et al.*, 2002; Sucuoğlu *et al.*, 2003]. The results illustrated in Fig. 4A show a direct relationship between the pattern of the

resonance frequency distribution and these three regions of Dinar. The resonance frequencies shown in Fig. 4A can also be classified into three groups, 0.3–1.0 Hz, 1.0–5.0 Hz, and 5.0–12.0 Hz, measured in the basin (zone III), transition (zone II), and hillside (zone I) regions, respectively. This zonation is similar to that made by Sucuoğlu *et al.* [2003]. The 1.0 and 5.0 Hz contours roughly correspond to the boundaries between the basin-transition and transition-hillside regions, respectively (Figs. 1 and 4A).

Hays [1986] suggested the relationship $T_b = N/10$ for estimating the natural period (T_b) of a building with N stories. The range of resonance frequencies of the soil in the basin region (zone III) is < 1.0 Hz, suggesting that only buildings with 10 or more stories have a resonance problem. However, no buildings this tall were present in the basin during the earthquake. The tallest buildings in the basin were 5–6 stories, which correspond to resonance frequencies of about 2 Hz. Consequently, these results suggest that no direct relationship exists between the resonance frequency and damage distribution in the basin region. Kayabali [1997] came to a similar conclusion using different data and speculated that the heavy damage likely resulted from the unusually long shaking duration, which was about 25 s. However, the resonance frequencies in the transition sites (zone II), which were between 1.0 and 5.0 Hz, are closer or equal to the natural periods of the buildings, which were mostly between two and five stories. The detailed damage report by Durukal *et al.* [1998] classified the damage to the one-, two-, four-, and five-story buildings as substantial to heavy, while most of the three-story buildings were destroyed. The shaded area in Fig. 1 indicates the areas with the greatest damage compiled from Durukal *et al.* [1998]. Although the resonance frequencies between 1.0 and 5.0 Hz seem to explain the damage in zone II (transition), those < 1.0 Hz fail to justify the damage in zone III (basin). Therefore, we need to seek other models that can explain the damage that occurred in both the basin and transition zones.

The shape of the Dinar basin played a key role in the long duration of shaking reported by Kayabali [1997]. It follows from Fig. 3C that the deepest part of the Dinar basin is in the middle and the sediments gradually get shallower to the east and west, where the basin is bounded by hills. The E-W length of the basin is 6–7 km. This basin shape may lead to the propagation of surface waves back and forth between the eastern and western hills. Analyzing the seismograms of the main shock and aftershocks, Yalcinkaya and Alptekin [2005] showed that arrivals following the direct S waves are surface waves generated at the edge of the Dinar basin. These late arrivals are featured by relatively large amplitudes and long durations, which are typical in the surface-wave train giving rise to long-period ground motions below 1.0 Hz (e.g., Kang and Baag, 2004a,b). Therefore, the damage distribution in Dinar during the 1995 earthquake can be predominantly attributed to the large amplitude and long duration of ground motions by the basin edge-induced waves, although we do not exclude the role of resonance effects between subsurface sediments and buildings. Further study on this problem, considering the effects of the three-dimensional basin geometry and the near-fault ground motions, is the subject of another ongoing study.

Acknowledgments

Tae-Seob Kang was supported by the Basic Research Project of KIGAM funded by the Ministry of Science and Technology of Korea. This study was supported by NATO Collaborative Linkage Grant Programme under Grant Number: EST.CLG.979847 and by the Research Fund of Istanbul University, project number UDP-2307/0204008.

This study was initially presented at Hazturk-2007, International Symposium on Earthquake Loss Estimation for Turkey.

References

- Ansal, A. M., Iyisan, R., and Gullu, H. [2001] "Microtremor measurements for the microzonation of Dinar," *Pure and Applied Geophysics* **158**, 2525–2541.
- Arai, H. and Tokimatsu, K. [2004] "S-wave velocity profiling by inversion of microtremor H/V spectrum," *Bulletin of the Seismological Society of America* **94**, 53–63.
- Bakir, B. S., Ozkan, M. Y., and Ciliz, S. [2002] "Effects of basin edge on the distribution of damage in 1995 Dinar, Turkey earthquake," *Soil Dynamics and Earthquake Engineering* **22**, 335–345.
- Bard, P. Y. and Chávez-García, F. J. [1993] "On the decoupling of surficial sediments from surrounding geology at Mexico city," *Bulletin of the Seismological Society of America* **83**, 1979–1991.
- Bodin, P., Smith, K., Horton, S., and Hwang, H. [2001] "Microtremor observations of deep sediment resonance in metropolitan Memphis, Tennessee," *Engineering Geology* **62**, 159–168.
- Cárdenas-Soto, M. and Chávez-García, F. J. [2003] "Regional path effects on seismic wave propagation in central Mexico," *Bulletin of the Seismological Society of America* **93**, 973–985.
- Carroll, D. L. [1996] "Genetic algorithms and optimizing chemical oxygen-iodine lasers," In: Wilson, H. B., Batra, R. C., Bert, C. W., Davis, A. M. J., Schapery, R. A., Stewart, D. S. and Swinson F. F. Eds. *Developments in Theoretical and Applied Mechanics*, Vol. 18, (School of Engineering, The University of Alabama, Tuscaloosa), pp. 411–424.
- Delgado, J., Casado, C. L., Estevez, A., Giner, J., Cuenca, A., and Molina, S. [2000a] "Mapping soft soils in the Segura river valley (SE Spain): a case study of microtremors as an exploration tool," *Journal of Applied Geophysics* **45**, 19–32.
- Delgado, J., Casado, C. L., Giner, J., Estevez, A., Cuenca, A., and Molina, S. [2000b] "Microtremors as a geophysical exploration tool: applications and limitations," *Pure and Applied Geophysics* **157**, 1445–1462.
- Dobry, R., Borcherdt, R. D., Crouse, C. B., Idriss, I. M., Joyner, W. B., Martin, G. R., Power, M. S., Rinne, E. E., and Seed, R. B. [2000] "New site coefficients and site classification system used in recent building seismic code provisions," *Earthquake Spectra* **16**, 41–67.
- Durukal, E., Erdik, M., Avci, J., Yuzugullu, O., Zulfukar, C., Biro, T., and Mert, A. [1998] "Analysis of the strong motion data of the 1995 Dinar, Turkey, earthquake," *Soil Dynamics and Earthquake Engineering* **17**, 557–578.
- Harkrider, D. G. [1964] "Surface waves in multilayered elastic media: Part 1," *Bulletin of the Seismological Society of America* **54**, 627–679.
- Hays, W. W. [1986] "Site amplification of earthquake ground motion," *Proceedings of the 3rd U.S. National Conference on Earthquake Engineering*, **1**, 357–368.
- Ibs-von Seht, M. and Wohlenberg, J. [1999], "Microtremor measurements used to map thickness of soft sediments," *Bulletin of the Seismological Society of America* **89**, 250–259.
- Kang, T.-S. and Baag, C. -E. [2004a] "Finite-difference seismic simulation combining discontinuous grids with locally variable timesteps," *Bulletin of the Seismological Society of America* **94**, 207–219.
- Kang, T.-S. and Baag, C. -E. [2004b] "An efficient finite-difference method for simulating 3D seismic response of localized basin structures," *Bulletin of the Seismological Society of America* **94**, 1690–1705.
- Kanli, A. I., Tildy, P., Prónay, Zs., and Pınar, A. [2004] "Quantitative Evaluation of Seismic Site Effects," Final Report, Nato Science Programme, Cooperative Science and Technology Sub-Programme, Collaborative Linkage Grant, Grant Number: EST.CLG.979847.
- Kanli, A. I., Tildy, P., Prónay, Zs., Pınar, A., and Hermann, L. [2006] " v_s^{30} mapping and soil classification for seismic site effect evaluation in Dinar region, SW Turkey," *Geophysical Journal International* **165**, 223–235.
- Kayabali, K. [1997] "The role of soil behaviour on damage caused by the Dinar earthquake (Southwestern Turkey) of October 1, 1995," *Environmental and Engineering Geoscience* **3**, 111–121.
- Luzon, F., Al Yuncha, Z., Sánchez-Sesma, F. J., and Ortiz-Aleman, C. [2001] "A numerical experiment on the horizontal to vertical spectral ratio in flat sedimentary basins," *Pure and Applied Geophysics* **158**, 2451–2461.

- Özpinar, B. [1978] "Geophysical Resistivity Investigation Report on the Afyon-Dinar Plain: 18th District of the State Hydraulic Works," Isparta, Turkey, 8p.
- Parolai, S., Bormann, P., and Milkereit, C. [2002] "New relationship between V_S , thickness of sediments, and resonance frequency calculated by the H/V ratio of seismic noise for the Cologne area (Germany)" *Bulletin of the Seismological Society of America* **92**, 2521–2527.
- Parolai, S., Picozzi, M., Richwalski, S. M., and Milkereit C. [2005] "Joint inversion of phase velocity dispersion and H/V ratio curves from seismic noise recordings using a genetic algorithm, considering higher modes," *Geophysical Research Letters* **32**, L01303, doi:10.1029/2004GL021115.
- Sabetta, F. and Bommer, J. [2002] "Modification of the spectral shapes and sub-soil conditions in Eurocode 8," *12th European Conference on Earthquake Engineering*, ref. 518.
- Satoh, T., Kawase, H., Iwata, T., Higashi, S., Sato, T., Irikura, K., and Huang, H. -C. [2001] "S-wave velocity structure of the Taichung basin, Taiwan, estimated from array and single-station records of microtremors," *Bulletin of the Seismological Society of America* **91**, 1267–1282.
- Scherbaum, F., Hinzen, K. G., and Ohrnberger, M. [2003] "Determination of shallow shear velocity profiles in the Cologne/Germany area using ambient vibrations," *Geophysical Journal International* **152**, 597–612.
- Sêco e Pinto, P. S. [2002] "Eurocode 8 - Design provisions for geotechnical structures," *3rd Croatian Conference on Soil Mechanical and Geotechnical Engineering 2002 Hvar*, CD-ROM.
- Street, R., Wang, Z., Woolery, E., Hunt, J., and Harris, J. [1997] "Site effects at a vertical accelerometer array near Paducah, Kentucky," *Engineering Geology* **46**, 349–367.
- Sucuoğlu, H., Anderson, J. G., and Zeng, Y. [2003] "Predicting intensity and damage distribution during the 1995 Dinar, Turkey, earthquake with generated strong motion accelerograms," *Bulletin of the Seismological Society of America* **93**, 1267–1279.
- Turker, E., Kaya, M. A., Kamaci, Z., Uyanik, O., Buyukkose, N., Mutluturk, M., Yalcin, A., and Ozkan, F. [1996] "Geotechnical Measurements at Dinar Disaster Region," General Directorate of Disaster Affairs and Suleyman Demirel University (a report in Turkish).
- Yalcinkaya, E. and Alptekin, Ö. [2005] "Contributions of basin-edge-induced surface waves to site effect in the Dinar basin, southwestern Turkey," *Pure and Applied Geophysics* **162**, 931–950.